Please cite this article in press as: Alazami et al., Mutations in *C2orf37*, Encoding a Nucleolar Protein, Cause Hypogonadism, Alopecia, Diabetes Mellitus, Mental Retardation, and..., The American Journal of Human Genetics (2008), doi:10.1016/j.ajhg.2008.10.018

ARTICLE

Mutations in *C2orf37*, Encoding a Nucleolar Protein, Cause Hypogonadism, Alopecia, Diabetes Mellitus, Mental Retardation, and Extrapyramidal Syndrome

Anas M. Alazami,[1] Amr Al-Saif,[1] Abdulaziz Al-Semari,[2] Saeed Bohlega,[2] Soumaya Zlitni,[1] Fatema Alzahrani,[1] Prashant Bavi,[3] Namik Kaya,[1] Dilek Colak,[4] Hanif Khalak,[1] Andy Baltus,[5] Borut Peterlin,[6] Sumita Danda,[7] Kailash P. Bhatia,[8] Susanne A. Schneider,[8] Nadia Sakati,[9] Christopher A. Walsh,[5] Futwan Al-Mohanna,[10] Brian Meyer,[1] and Fowzan S. Alkuraya[1,5,11,*]

Hypogonadism, alopecia, diabetes mellitus, mental retardation, and extrapyramidal syndrome (also referenced as Woodhouse-Sakati syndrome) is a rare autosomal recessive multisystemic disorder. We have identified a founder mutation consisting of a single base-pair deletion in *C2orf37* in eight families of Saudi origin. Three other loss-of-function mutations were subsequently discovered in patients of different ethnicities. The gene encodes a nucleolar protein of unknown function, and the cellular phenotype observed in patient lymphoblasts implicates a role for the nucleolus in the pathogenesis of this disease. Our findings expand the list of human disorders linked to the nucleolus and further highlight the developmental and/or maintenance functions of this organelle.

Introduction

Hypogonadism, alopecia, diabetes mellitus, mental retardation, and extrapyramidal syndrome, also known as Woodhouse-Sakati syndrome (WSS [MIM 241080]), is a rare autosomal recessive disorder originally described in a number of consanguineous Saudi families, but which has recently been reported in other ethnicities as well[1–4] (Figures 1A and 1B). Additional manifestations include sensorineural deafness, decreased signal intensity in the basal ganglia, T-wave abnormalities, and depressed insulin-like growth factor 1 (IGF-1) levels.[5] The number of organs involved clinically and the progressive nature of their involvement suggest that the discovery of the genetic defect underlying this syndrome will enhance our understanding of the development and/or maintenance of these organs. In this study, we used linkage analysis followed by sequencing to uncover the gene responsible for this multisystemic disorder. Our data revealed a common founder mutation in *C2orf37* as the cause of WSS in all the Saudi families we examined, including the ones originally described by Woodhouse and Sakati. Subsequent analysis of WSS patients from other ethnicities identified three additional mutations in *C2orf37*. We show that this gene encodes a previously uncharacterized nucleolar protein and that nucleoli of patient lymphoblasts display enhanced sensitivity to transcriptional blockade.

Materials and Methods

Patients

All patients or their legal guardians provided written and informed consent according to a protocol approved by the institutional review board of the institution wherein blood samples were taken, in adherence to the Helsinki guidelines.

Linkage Analysis

Low-resolution whole-genome scan was initially performed with the Human Marker Panel v.8a (Research Genetics). Multipoint linkage analysis was performed with GeneHunter (v.1.2), and a 100% penetrant autosomal recessive trait was assumed, with a frequency of 0.0001 (rare disease) and equal allele frequency for all microsatellite markers. This scan identified a region of extended homozygosity on chromosome 2q between markers D2S1399 and D2S434. Additional families were genotyped, and fine mapping subsequently reduced the critical region to 1.2 Mb; the centromeric border was defined by a dinucleotide repeat polymorphism in intron 2 of the *TLK1* gene (MIM 608438) and the telomeric border by marker D2S326.

Mutation Detection

Primers were designed to flank the coding regions of all genes in the mapped interval, and direct sequencing was performed with the dideoxy chain-termination method (Amersham ET Dye Termination Sequencing Kit), with samples being processed on a MegaBACE1000 (Molecular Dynamics). Sequence analysis was undertaken with SeqMan II (DNASTAR). Mutations described in

[1]Department of Genetics, King Faisal Specialist Hospital and Research Center, Riyadh 11211, Saudi Arabia; [2]Department of Neurosciences, King Faisal Specialist Hospital and Research Center, Riyadh 11211, Saudi Arabia; [3]Biological Repository Section, King Faisal Specialist Hospital & Research Center, Riyadh 11211, Saudi Arabia; [4]Department of Biostatistics and Scientific Computing, King Faisal Specialist Hospital and Research Center, Riyadh 11211, Saudi Arabia; [5]Division of Genetics and Metabolism, Department of Medicine, Children's Hospital Boston and Harvard Medical School, Boston, MA 02115, USA; [6]Institute of Medical Genetics, Department of Obstetrics & Gynecology, University Medical Center Ljubljana, 1000 Ljubljana, Slovenia; [7]Clinical Genetics Unit, Christian Medical College and Hospital, Vellore 632004, Tamil Nadu, India; [8]Sobell Department, Institute of Neurology, University College London, Queen Square, London WC1N 3BG, UK; [9]Department of Pediatrics, King Faisal Specialist Hospital and Research Center, Riyadh 11211, Saudi Arabia; [10]Department of Cell Biology, King Faisal Specialist Hospital and Research Center, Riyadh 11211, Saudi Arabia; [11]Department of Pediatrics, King Khalid University Hospital and College of Medicine, King Saud University, Riyadh 11461, Saudi Arabia
*Correspondence: falkuraya@kfshrc.edu.sa
DOI 10.1016/j.ajhg.2008.10.018.

Please cite this article in press as: Alazami et al., Mutations in *C2orf37*, Encoding a Nucleolar Protein, Cause Hypogonadism, Alopecia, Diabetes Mellitus, Mental Retardation, and..., The American Journal of Human Genetics (2008), doi:10.1016/j.ajhg.2008.10.018

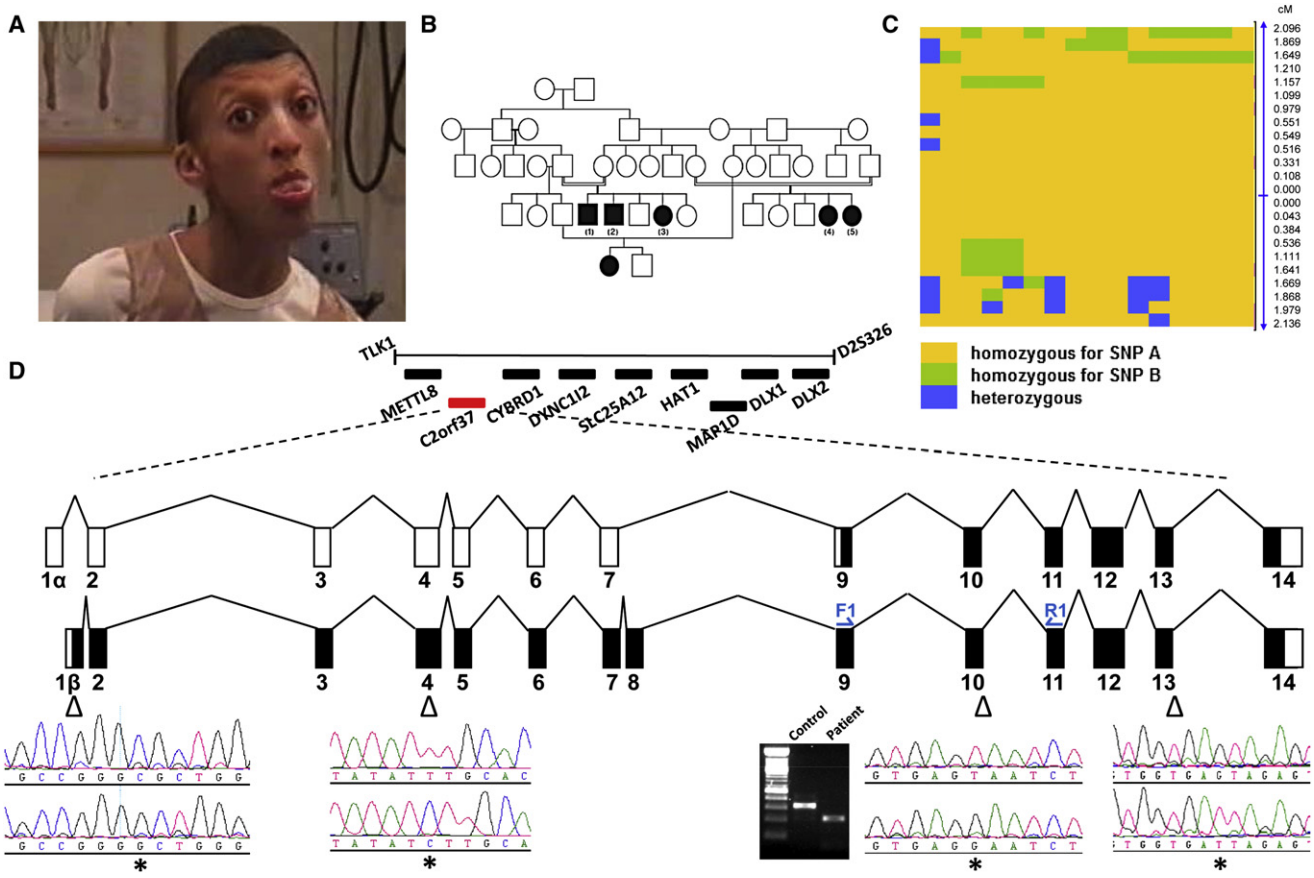

Figure 1. *C2orf37* Mutations Are Responsible for Woodhouse-Sakati Syndrome

(A) WSS patient with dystonia and alopecia.

(B) One illustrative WSS pedigree showing multiple consanguinity loops.

(C) Haplotype analysis of Saudi WSS patients. Each column represents one of the 18 patients studied, and each row represents one of the SNPs used for the analysis. Color codes specify the genotypes of each SNP as AA, BB, or AB, and the genetic distance of each SNP from *C2orf37* is listed to the right.

(D) Critical linkage interval obtained after fine mapping, with *C2orf37* in red. The two major isoforms are shown as well, with open boxes representing untranslated regions and shaded boxes representing the coding sequences (not drawn to scale). The ORFs are in-frame and utilize the same stop codon. Chromatograms of the four mutations show control sequences on top, with mutations denoted by asterisks. Arrowheads indicate location within the gene. RT-PCR analysis (using F1 and R1 primers) of a normal control and one WSS patient from (4) reveals skipping of exon 10 in the latter.

the text are based on Accession NM_025000.2. All primer sequences are available from the authors upon request.

Haplotyping

For discovering the minimal interval of homozygosity for the Saudi founder mutation, the haplotypes of 18 patients from eight unrelated families were assessed with single-nucleotide polymorphism (SNP)-specific primers. SNPs were spaced roughly 200 Kb apart for 3 Mb on either side of *C2orf37*. Calculating the mutation's age was as described.[6]

Characterization of Splice Isoforms

cDNA was synthesized from 1 μg of total lymphocyte RNA with the First Strand Synthesis Kit (Promega) and random hexamers. This was then PCR amplified with primers specific for exon 1α and exon 14 or exon 1β and exon 14. The end product was TA cloned (Invitrogen), and individual colonies were picked and sequenced for establishing a catalog of splice variants.

GFP-Fusion and Overexpression Constructs

For the GFP-fusion experiment, a full-length open reading frame (ORF) of the β-isoform was subcloned into peGFP-C1 (Clontech) and then sequenced bidirectionally for ensuring the absence of PCR artifacts. For overexpression studies without the use of a fusion tag, the same ORF was subcloned into pAsc (a kind gift from Khalid Abu Khabar), allowing expression of exogenous protein under a cytomegalovirus promoter.

Cell Culture

HEK293 cells were maintained under standard conditions in Dulbecco's modified Eagle's medium supplemented with 10% fetal bovine serum, 100 units/ml of penicillin/streptomycin, and L-glutamine. Epstein-Barr virus (EBV)-transformed lymphoblasts were maintained in RPMI supplemented with 20% fetal bovine serum and 200 units/ml of penicillin/streptomycin. For transfection experiments, HEK293 cells were cultured in six-well dishes on coverslips coated with Poly-L-Lysine (Sigma) and transfected

with SuperFect (QIAGEN) according to the manufacturers' instructions.

Real-Time Reverse Transcriptase-Polymerase Chain Reaction

A suite of first-strand cDNA from 48 adult, healthy human tissues was purchased from Origene. Primers specifically interrogated the abundance of exon 1α versus exon 1β cDNA. Reactions were performed in a LightCycler (Roche), and PCR products were subsequently assessed via melt-curve analysis and gel electrophoresis.

Antibody Production

Production of the C2orf37 rabbit polyclonal antibody was outsourced to Abgent. The antigenic sequence FNLLDDDPEQETFKI corresponds to amino acids 412–426 of the protein (Accession NP_079276.2), and the antibody was delivered after affinity-column purification along with the synthetic antigen.

Immunohistochemistry

Mouse embryo tissue slides were purchased from Zyagen. After antigen retrieval, slides were processed with the streptavidin-biotin peroxidase technique, and diaminobenzidine (DAB) was used as chromogen. The sections were incubated overnight in a 1:1000 dilution of anti-C2orf37, and the Dako Envision Plus System kit was used as the secondary detection system, with DAB as chromogen. Endogenous peroxidase activity was quenched with 3% hydrogen peroxidase in methanol. Endogenous biotin was blocked, and all slides were counterstained with hematoxylin, dehydrated, cleared, and coverslipped with premount. A cell-line block of HEK293 cells served as a positive control. Two types of negative controls were used: The first was the exclusion of the primary antibody, and the second was a peptide competition assay. For the latter, anti-C2orf37 was preincubated with the peptide antigen (Abgent) at a 1:2 ratio (w/w) for 1 hr at room temperature, prior to staining.

Tissue Section In Situ Hybridization

RNA extracted from flash-frozen adult mouse liver (RNeasy Mini Kit, QIAGEN) was used as template for synthesizing two PCR products specific for *4833418A01Rik*, the *C2orf37* mouse ortholog (SuperScript One-Step RT-PCR, Invitrogen). The first of these PCR products corresponded to an 871 base pair (bp) fragment beginning at c.46 (Accession AK160679.1), and the second corresponded to an 894 bp fragment starting at c.1076. PCR primers were tagged with T7 or SP6 sequences. Sense and antisense digoxygenin-labeled RNA probes were prepared with the MaxiScript Kit (Ambion) and Roche's DIG RNA Labeling Mix. Mouse embryo tissue slides from Zyagen were heated to 45°C (30 min), allowed to cool to room temperature, twice dewaxed in xylene (15 min each), and then rehydrated. All subsequent steps were performed with the InsituPro VSi (Intavis) in accordance with a manufacturer-recommended protocol. Samples were twice permeabilized with proteinase K (10 μg/ml) at 37°C for 10 min each, hybridized to the probe for 12 hr at 65°C, and incubated with alkaline-phosphatase-coupled digoxygenin antibody (Roche) at room temperature for 4 hr. Full details are available from the authors upon request. Slides were finally incubated in BM Purple (Roche) until appropriate color development.

Immunofluorescence

HEK293 cells grown on coverslips were fixed with prewarmed 3.6% formaldehyde, then permeabilized with 0.5% Triton X-100 (Sigma). Mouse monoclonal anti-B23 was purchased from Abcam (ab10530). After 1 hr incubation with primary antibody at room temperature, cells were incubated for another hour in rhodamine- or flourescein-labeled goat anti-mouse or anti-rabbit IgG (Pierce), then observed under a fluorescent microscope (Zeis). Lymphoblasts were treated as above, except that all incubations were carried out in suspension, and cells were centrifuged at 3000 g for 2 min between steps. The peptide competition assay was performed as described for immunohistochemistry.

Drug Treatment

For the selective inhibition of RNA polymerase I-catalyzed transcription, HEK293 cells and lymphoblasts were treated with 0.05 μg/ml actinomycin D (Sigma) for 3 hr prior to fixation. For full inhibition of cellular transcription, this was increased to 10 μg/ml.

Gene-Expression Profiling

Total RNA was extracted from two unrelated normal control lymphoblast cell lines and three unrelated patient lymphoblast cell lines with standard protocols. Sample handling, cDNA synthesis, cRNA labeling and synthesis, hybridization, washing and scanning of chips, and all related quality controls were performed according to manufacturer's instructions (Affymetrix). Two replicates of each sample were run on Affymetrix GeneChip Human Genome U133 Plus 2.0 Arrays. Statistical analyses were performed with MATLAB (The Math Works) and the PARTEK Genomics Suite (Partek software v.6.3, Partek). Significantly modulated genes were defined as those with an absolute fold change >2 and an unadjusted p value <0.006.

Results

Mutations in *C2orf37* Cause WSS

A genome-wide linkage analysis on three affected siblings from one of the original Saudi families identified an extended autozygous region encompassing chromosome 2q22.3–2q35. Inclusion of another family with four affected siblings confirmed the homozygosity and yielded a maximum multipoint LOD score of 6.13 from markers D2S2284 to D2S1791. Fine mapping further narrowed the critical region to 1.2 Mb; the centromeric border was defined by a dinucleotide repeat polymorphism in intron 2 of the TLK1 gene and the telomeric border by marker D2S326. This region contains a total of 13 genes and pseudogenes, both known and predicted (Figure 1D). Sequencing of a hypothetical gene, *C2orf37*, revealed the only mutation we found within this interval: a 1 bp deletion that fully segregated with the phenotype (c.436 delC; see Methods for numbering scheme) (Figure 1D). The same mutation was uncovered in six additional Saudi families but was not found in 274 Saudi control chromosomes. To address doubts that *C2orf37* might simply be a pseudogene segregating perfectly with the disease locus, we sequenced all putative coding segments of this gene in

at least 184 normal Saudi chromosomes, and no truncating mutations were found. SNP-based haplotype analysis confirmed that this is a founder mutation, with a haplotype interval of 1.1 Mb shared between 18 Saudi patients (Figure 1C). Calculations based on a simplified likelihood algorithm[6] suggest a maximal probability that this mutation arose approximately 55 generations ago.

Analysis of this gene has revealed extreme splicing variability, and, from lymphocytes alone, we have isolated at least 30 different isoforms that vary greatly in abundance (data not shown). Our common mutation resides in exon 4 but is not likely to be pathogenic for every splice form. We have identified at least two major isoforms of roughly equal abundance, each bearing a different initiation site. In the first of these (henceforth referred to as the α-isoform), the 1 bp deletion is predicted to lie in the 5′UTR and so is unlikely to be pathogenic, whereas in the other (which we here refer to as the β-isoform), it resides within the ORF and is predicted to cause a frameshift (p.Ala147HisfsX9; Accession NP_079276.2) (Figure 1D). Subsequent analysis of WSS patients from other ethnicities revealed three additional mutations in this gene. A sporadic patient of Eastern European descent[2] harbored a 1 bp deletion that again predicts a frameshift in the β-isoform only (c.50 delC). The other two mutations affect splice donor sites: An Indian family with three affected individuals[1] carried a c.1422+5G > T mutation, whereas two affected siblings of Middle Eastern origin[4] displayed the mutation c.1091+6T > G. These splice-site mutations are predicted to be pathogenic for both major transcripts. The latter (Middle Eastern) mutation was confirmed to result in the skipping of exon 10, leading to a frameshift (Figure 1D). The Indian mutation changes the GTGAGT consensus-donor sequence to GTGATT and is predicted to result in a dramatic drop in splicing efficiency (from 0.95 to 0.06, according to the Berkeley *Drosophila* Genome Project, and from 0.81 to 0.0, according to the NetGene2 Server). All patients from all ethnicities were homozygous for their respective mutations. As a further check, ethnically matched normal controls were screened for each of the three non-Saudi mutations: The Middle Eastern mutation was screened against 250, the Slovenian against 210, and the Indian against 196 control chromosomes. As with the Saudi mutation, none of the controls was found to be a carrier. These independent mutations provide compelling evidence that aberrations in *C2orf37* underlie this syndrome.

C2orf37 Encodes a Nucleolar Protein

Virtually nothing is known about *C2orf37* or the proteins it encodes. The β-isoform encompasses the longest possible ORF, predicting a 520 amino acid protein that does not contain any recognized domain or localization signal and that shares no significant homology with other proteins. This putative amino acid sequence is well conserved across species, however, with orthologs (also hypothetical) present in the mouse, rat, chimpanzee, cow, fowl, and other higher animals (expect value = 0.0). In humans, the predicted peptide for the α-isoform is identical to the last 240 residues of the β-isoform protein, given that the two ORFs are in-frame and utilize the same stop codon (Figure 1D). Real-time RT-PCR analysis of various adult human tissues revealed low ubiquitous expression of both isoforms in all tissues examined (data not shown). With an aim to further characterize the proteins, we raised a polyclonal antibody against a synthetic peptide representing a hydrophilic stretch of 15 amino acids encoded by exon 12. This stretch is shared by the putative peptides of both the α-isoform and β-isoform. Immunohistochemistry using this antibody revealed nearly ubiquitous nucleolar expression for *C2orf37* in mouse embryos, with regions of enhanced staining in the brain, liver, and skin tissues (Figures 2A–2C). There was no appreciable staining of islet cells at the developmental stages examined, however (E16.5 mouse embryo and adult human pancreas). Preincubating the antibody with the peptide antigen abrogated the nucleolar staining and thus confirmed specificity of the signal (Figure 3). As a companion experiment, we also performed in situ hybridization on mouse embryo sections to assess the RNA expression profile for *4833418A01Rik*, the mouse ortholog of *C2orf37*. Two sense and two antisense probes were used for this purpose. The staining patterns for both antisense probes were analogous to the results obtained through immunohistochemistry, with *4833418A01Rik* transcription most evident in the brain, liver, and skin tissues (Figures 2D–2F). The intensity of staining in the brain was comparatively weak when evaluated against the other two tissues, although this is in line with the data provided by the Allen Brain Atlas for this gene. As a negative control, the two sense probes generated only nonspecific staining, as expected (data not shown). These RNA and protein staining patterns are biologically relevant given that WSS patients manifest CNS abnormalities, alopecia, and low IGF-1 (liver hormone).[5]

Given the lack of any conserved domains or clear localization signals, we set out to assess the cellular activity of C2orf37 through the use of a GFP-fusion construct transfected into HEK293 cells. Intriguingly, expression of the fusion protein resulted in disruption of the nuclear membrane and the aggregation of the fusion protein into a large globular structure displacing the nucleus, probably an artifact indicative of toxicity (data not shown). In lieu of meaningful GFP-fusion data, the two major isoforms of C2orf37 were exogenously expressed in HEK293 without fusion to any tags and then detected with our antibody. Overexpression of both α-protein and β-protein isoforms demonstrated nucleolar localization, in line with our immunohistochemistry findings (Figures 4A–4C). We also explored the localization of the endogenous protein in untransfected cells, and here, too, our antibody specifically recognized nucleoli in accordance with our immunohistochemistry data. This was confirmed through colocalization of the endogenous C2orf37 with B23 (nucleophosmin), a known marker of the granular component of

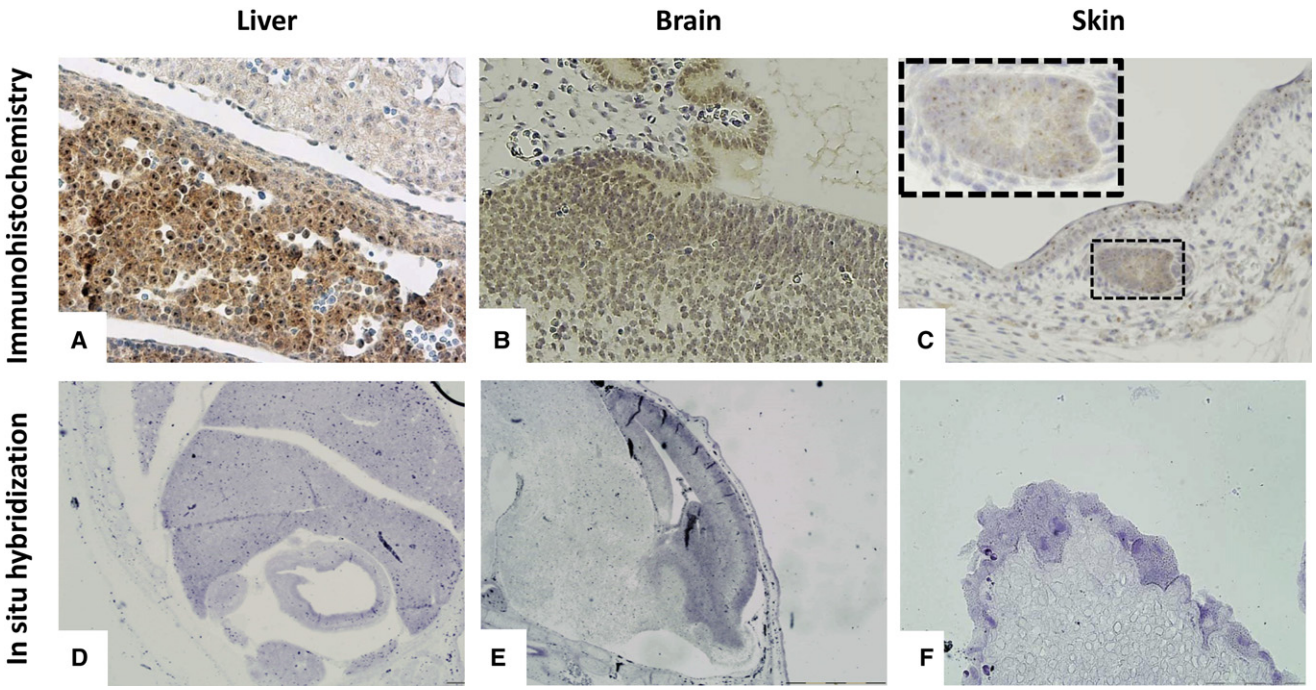

Figure 2. Immunohistochemistry and In Situ Hybridization on Mouse Embryonic Tissues
Intense nucleolar staining of hepatocytes (heart tissue is visible in the upper right corner) at E16.5 (A), brain cells at E12.5 (B), and different layers of skin including a hair follicle (inset) at E14.5 (C). Bottom panels present in situ hybridization patterns observed for liver tissue at E13.5 (D), cortex of the brain at E15.5 (E), and skin at E15.5 (F).

the nucleolus[7] (Figures 4D–4F). Again, preincubation of the antibody with the peptide antigen resulted in complete loss of this staining, whereas, as a positive control, the GFP-fusion protein in transfected HEK293 cells was found to colocalize perfectly with anti-C2orf37 staining (data not shown). These results further verified antibody specificity.

Nucleoli in Patient Lymphoblasts Have Enhanced Sensitivity to Transcriptional Blockade

To further interrogate the function of C2orf37, we subjected HEK293 cells to low and high doses of actinomycin D, a powerful inhibitor of transcription. The low dose selectively blocks the nucleolar RNA polymerase I only, whereas the high dose impedes all transcriptional activity in the cell.[8] We discerned that at the lower dosage, C2orf37 mostly retains its nucleolar compartmentalization, whereas B23, involved in ribosome biogenesis among other functions, diffuses fully into the nucleoplasm. Surprisingly, although the higher dosage does induce C2orf37 translocation to the nucleoplasm, a minority of cells continues to retain it in the nucleolus (Figure 5). Our findings hence suggest that the nucleolar localization of C2orf37 is only partially dependant on active transcription.[9]

To assess the effects of the founder mutation, we compared lymphoblasts from Saudi patients and controls and found that patient lymphoblasts consistently

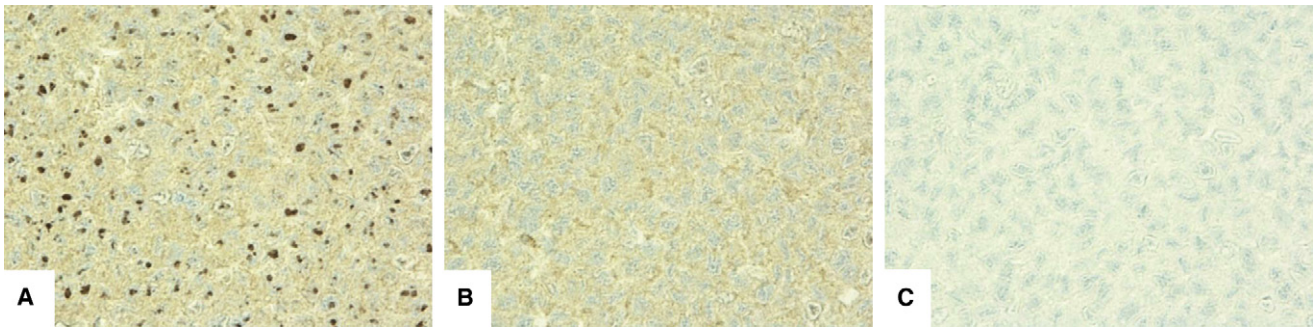

Figure 3. Nucleolar Staining of C2orf37 Is Specific
(A) Immunohistochemistry on paraffin sections of a HEK293 cell block showing strong nucleolar and weak cytoplasmic staining.
(B) Nucleolar but not cytoplasmic staining is abrogated when the slide is incubated with the peptide antigen prior to staining with C2orf37 antibody.
(C) Buffer negative control, with the primary antibody excluded.

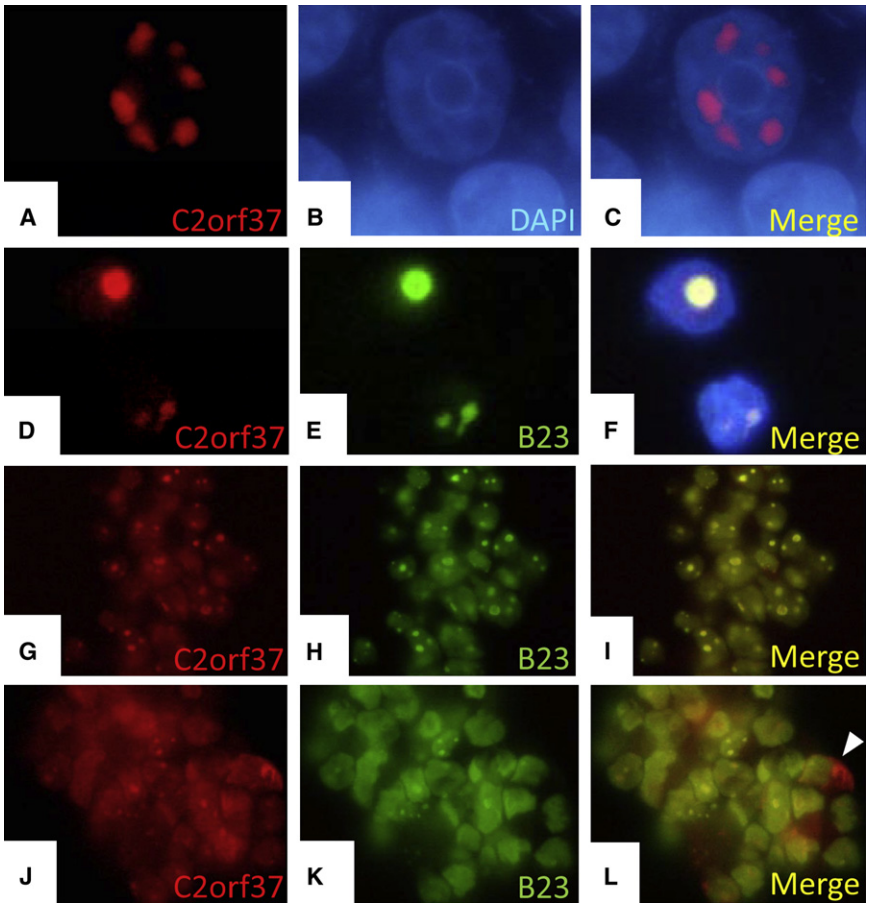

Figure 4. Both Major Isoforms of C2orf37 Localize to the Nucleolus in Tissue Culture

(A–C) Overexpression of the β-isoform protein from a cloned expression construct results in nucleolar localization of the peptide in HEK293 cells. The same pattern appears for the α-isoform.

(D–F) Endogenous C2orf37 colocalizes with B23, a nucleolar marker, in lymphoblasts.

(G–L) C2orf37 and B23 remain largely nucleolar after low-dose actinomycin D treatment of control lymphoblasts (G–I), but largely nucleoplasmic in patient lymphoblasts (J–L), where their colocalization is partially lost (indicated by arrowhead).

demonstrated enhanced sensitivity to the transcriptional blockade induced by low actinomycin D concentration. This was evident from the loss of nucleolar staining of both B23 and C2orf37 in a majority of actinomycin D-treated patient lymphoblasts, in contrast to an opposite trend observed in control cells (Figures 4G–4L).

Discussion

In this study we have shown that mutations in *C2orf37* cause the hypogonadism, alopecia, diabetes mellitus, mental retardation, and extrapyramidal syndrome described by Woodhouse and Sakati in 1983. As can be inferred from the pleiotropic nature of the disorder, the expression profile of C2orf37 is wide but relevant to the clinical manifestations, given that we have demonstrated pockets of increased expression in the brain, liver, and skin. Weak expression has also been seen in seminiferous tubules, but no convincing expression could be seen in islet cells. The latter could be attributed to the limited number of developmental stages examined immunohistochemically (E16.5 mouse embryo and adult human), although in situ analysis of multiple embryo stages demonstrated similar absence of islet cell staining. Despite the apparent lack of any clear localization signal, the *C2orf37* proteins that we tested have consistently been detected in the nucleoli. Our hypothesis that a nucleolar defect may underlie the pathogenesis of WSS was further substantiated by the nucleolar hypersensitivity of patient lymphoblasts to transcriptional blockade. Similar hypersensitivity to actinomycin D has been recently reported in Diamond-Blackfan anemia, a distinct but similarly pleiotropic autosomal recessive disorder.[10] Although it may be tempting to speculate that defective ribosome biogenesis is the pathogenic mechanism in WSS, this cellular phenotype has to be viewed in the context that long-term inhibition of RNA polymerase I blocks not only rRNA transcription, but subsequently the assembly of the nucleolus itself by impeding the fusion of prenucleolar bodies (PNBs) and the nucleolar organizer regions (NORs).[8] Therefore, actinomycin D may be unmasking an assembly defect, and so we cannot discard the possibility that other nucleolar functions, which include regulation of cell cycle, cellular aging, signal-recognition-particle biosynthesis, small-RNA processing, mRNA transport, and even apoptosis,[11,12] may underlie the pathogenesis of WSS. Indeed, when we compare the expression signature of control and patient lymphoblasts, we observe significant differential expression of genes involved in apoptosis (data not shown). Very recently, Nousbeck et al. reported in this journal that a syndrome characterized by alopecia, neurological defects, and endocrinopathy is caused by decreased expression of RBM28, a nucleolar protein associated with ribosome biogenesis.[13] Although that syndrome and WSS are distinguishable clinically, our implication of a nucleolar protein in the pathogenesis of WSS strongly suggests that the clinical similarity between the two syndromes may reflect an overlapping molecular defect. Given the pleiotropic nature of WSS, analysis of *C2orf37* promises to shed light on the ill-defined role of the nucleolus in the development

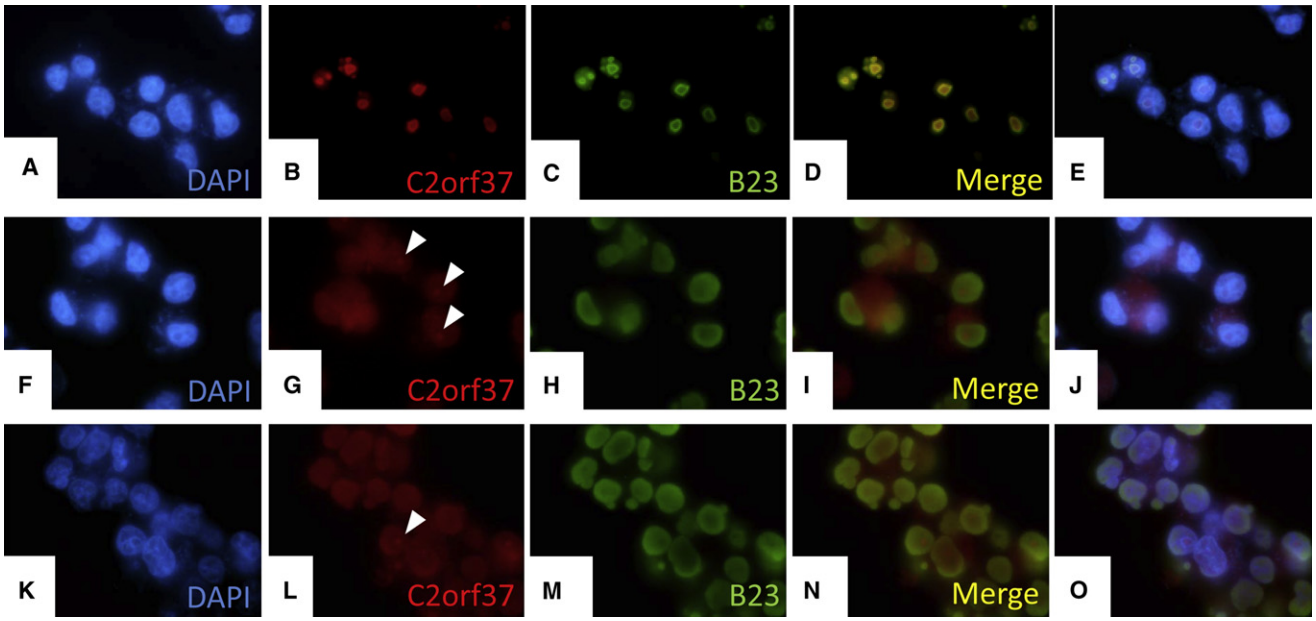

Figure 5. Nucleolar Localization of C2orf37 in HEK293 Cells Is Less Dependent than B23 on Active Transcription
(A–E) C2orf37 and B23 colocalize at the nucleolus under normal conditions in HEK293 cells.
(F–J) Low-dose actinomycin D treatment results in full displacement of B23 but only partial displacement of C2orf37 to the nucleoplasm (arrowheads point to foci of retained nucleolar localization).
(K–O) High-dose actinomycin D results in a similar but more potent effect, given that less foci of retained C2orf37 nucleolar localization can be seen.

and/or maintenance of multiple key organs such as the liver and brain.

Acknowledgments

We are grateful to the family members for their enthusiastic and generous participation. We thank Mohammad Rajab and Shamsa Al-Enazi for help with DNA sequencing and genotyping, Abdullah Al-Jeffrey and Ranad Shaheen for expert technical assistance, Tarfa Al-Sheddi for EBV transformation of lymphocytes, AlBandary AlBakheet for RNA sample processing (gene-expression profiling), Osama Alsmadi and Osama Al-Dirbashi and their respective teams for help in acquiring normal controls, and Khalid Abu Khabar and Azhar Hussain for helpful discussions throughout the course of research. We would also like to thank Salma M. Wakil and Batoul Baz for their help in processing Affy U133 chips. This study was approved and funded by the King Faisal Specialist Hospital and Research Centre (RAC#203-0037).

Received: August 19, 2008
Revised: October 20, 2008
Accepted: October 21, 2008
Published online: November 20, 2008

Web Resources

The URLs for data presented herein are as follows:

Allen Brain Atlas, http://www.brain-map.org
Berkeley *Drosophila* Genome Project (splice-site prediction), http://www.fruitfly.org/seq_tools/splice.html
Entrez Nucleotide, http://www.ncbi.nlm.nih.gov/sites/entrez?db=nucleotide
Entrez Protein, http://www.ncbi.nlm.nih.gov/sites/entrez?db=protein
NetGene2 Server, http://www.cbs.dtu.dk/services/NetGene2
Online Mendelian Inheritance in Man (OMIM), http://www.ncbi.nlm.nih.gov/omim

References

1. Koshy, G., Danda, S., Thomas, N., Mathews, V., and Viswanathan, V. (2008). Three siblings with Woodhouse-Sakati syndrome in an Indian family. Clin. Dysmorphol. *17*, 57–60.
2. Medica, I., Sepcic, J., and Peterlin, B. (2007). Woodhouse-Sakati syndrome: Case report and symptoms review. Genet. Couns. *18*, 227–231.
3. Woodhouse, N.J., and Sakati, N.A. (1983). A syndrome of hypogonadism, alopecia, diabetes mellitus, mental retardation, deafness, and ECG abnormalities. J. Med. Genet. *20*, 216–219.
4. Schneider, S.A., and Bhatia, K.P. (2008). Dystonia in the Woodhouse Sakati syndrome: A new family and literature review. Mov. Disord. *23*, 592–596.
5. Al-Semari, A., and Bohlega, S. (2007). Autosomal-recessive syndrome with alopecia, hypogonadism, progressive extrapyramidal disorder, white matter disease, sensory neural deafness, diabetes mellitus, and low IGF1. Am. J. Med. Genet. A *143*, 149–160.
6. Genin, E., Tullio-Pelet, A., Begeot, F., Lyonnet, S., and Abel, L. (2004). Estimating the age of rare disease mutations:

The example of Triple-A syndrome. J. Med. Genet. *41*, 445–449.

7. Boisvert, F.M., van Koningsbruggen, S., Navascués, J., and Lamond, A.I. (2007). The multifunctional nucleolus. Nat. Rev. Mol. Cell Biol. *8*, 574–585.
8. Ochs, R.L., Lischwe, M.A., Shen, E., Carroll, R.E., and Busch, H. (1985). Nucleologenesis: Composition and fate of prenucleolar bodies. Chromosoma *92*, 330–336.
9. Utama, B., Kennedy, D., Ru, K., and Mattick, J.S. (2002). Isolation and characterization of a new nucleolar protein, Nrap, that is conserved from yeast to humans. Genes Cells *7*, 115–132.
10. Ganapathi, K.A., Austin, K.M., Lee, C.S., Dias, A., Malsch, M.M., Reed, R., and Shimamura, A. (2007). The human Shwachman-Diamond syndrome protein, SBDS, associates with ribosomal RNA. Blood *110*, 1458–1465.
11. Dousset, T., Wang, C., Verheggen, C., Chen, D., Hernandez-Verdun, D., and Huang, S. (2000). Initiation of nucleolar assembly is independent of RNA polymerase I transcription. Mol. Biol. Cell *11*, 2705–2717.
12. Kerr, L.E., Birse-Archbold, J.L., Short, D.M., McGregor, A.L., Heron, I., Macdonald, D.C., Thompson, J., Carlson, G.J., Kelly, J.S., McCulloch, J., and Sharkey, J. (2007). Nucleophosmin is a novel Bax chaperone that regulates apoptotic cell death. Oncogene *26*, 2554–2562.
13. Nousbeck, J., Spiegel, R., Ishida-Yamamoto, A., Indelman, M., Shani-Adir, A., Adir, N., Lipkin, E., Bercovici, S., Geiger, D., van Steensel, M.A., et al. (2008). Alopecia, neurological defects, and endocrinopathy syndrome caused by decreased expression of RBM28, a nucleolar protein associated with ribosome biogenesis. Am. J. Hum. Genet. *82*, 1114–1121.